STOCHASTIC SCENARIO BASED MICROGRID ENERGY MANAGEMENT WITH ELECTRIC VEHICLES CONSIDERING UNCERTAINTY SOURCES

Mahmoudreza GHADI-SAHEBI[1], Reza EBRAHIMI[2]

This paper focuses on energy management of distributed generation sources and electric vehicles in a grid-connected microgrid considering uncertainties. The problem is formulated as a multi-objective optimization problem of energy cost and emission. In this context, innovative scenario-based objective functions are introduced to handle different uncertainties in the microgrid energy management. Since the objective functions are based on scenarios, appropriate probability density functions for each uncertainty source are defined, and then scenarios are randomly generated to be included in the objective function. To solve the optimization problem, the modified version of the multi-objective particle swarm optimization (MOPSO) algorithm is used. Also, the multiple-objective genetic algorithms and the multiple-objective differential evolution algorithms are used for optimization. The results confirm the effectiveness of objective functions and the good performance of the proposed modified MOPSO algorithm.

Keywords: Microgrid; Electric Vehicles; Multi-Objective Optimization; Uncertainty

1. Introduction

One of the most important issues in the Microgrid (MG) field is the environmental pollution and the costs of power generation, which should be carefully considered. The energy management of distributed generation (DG) sources and electric vehicles (EVs) in the MG were studied using the network load curve and time-varying electricity prices during the day [1]. EV charging is mainly shifted to off-peak times when electricity is cheap, and the use of EV discharge and DGs schedule for peak-load times. Therefore, the presence of DGs and EV parking lots can improve the network power quality, if energy management is done correctly [2]. On the other hand, many uncertainties need to be considered in the MG field. The uncertainties indicate the lack of accurate information related to the parameter values of system components, and measurements. The most important uncertainty sources in the MG include: loading condition, wind speed, power, solar generation and the uncertainty related to EVs [3].

[1] Department of Electrical Engineering, Gorgan Branch, Islamic Azad University, Gorgan, Iran, e-mail: M.ghadi@gorganiau.ac.ir

[2] Department of Electrical Engineering, Gorgan Branch, Islamic Azad University, Gorgan, Iran, e-mail: R.ebrahimi@gorganiau.ac.ir (Corresponding Author)

Researchers have shown that more than 90% EVs are mostly unused in the park mode [4]. Considering the charge stations for connecting EVs to the MG, can provide an additional power under the name of vehicle-to-grid (V2G) at peak times. This solution can be implemented by discharging EV batteries at peak hours and charging them at other times. EVs have plenty of economic and environmental benefits, but they provide more complexity for planning and operation of the power network. Therefore, EVs integration in a MG requires the new computational methods [5]. A daily model of energy resource planning for smart grids is proposed in the presence of a large number of EVs. In this research work, a new demand response method, which reduced the energy consumption by changing the travel plans, was introduced [6]. A charging method is studied for EV owners. In this study, by controlling the charge and discharge time of the EVs, the profitability and consent of EV owners is obtained [7]. A planning method using EVs in the MG is proposed. The proposed planning method focuses on the environmental and economic issues with the aim of integrating a large number of EVs into the MG by considering uncertainty sources [8]. An optimal EV charge and discharge considering the uncertainty of EV and WT was studied. Based on the possible behavior of EVs and WT, the objective function was defined to reduce cost and emission [9]. A real-time load management approach to coordinate the charging EVs in a distribution system was used. This strategy is based on minimizing the total energy production cost and the energy losses cost of a distribution system [10]. A new management method for estimating the electric energy consumption of EVs is presented. In this study assumed that a certain percentage of EVs are in the charging mode. In this method, by managing the charging and discharging time of EVs at charging stations, the optimum points for lowest cost and emissions were obtained [11]. In another study, a new load management strategy for optimizing the charging EVs was proposed for the peak-shaving of load curve [12]. The role of EVs in demand side management and network balancing for a MG was investigated. Moreover, incentive factors for the charging EVs were considered. The results showed that EV owners, is generally benefit from these conditions [13]. A new method for load management was proposed to coordinate the charge of several EVs in the MG for improving the network reliability and minimize the total cost of purchasing or selling energy for charging and discharging EVs. The proposed method reduces the production cost through considering the uncertainty of energy market prices and the charging time of EVs [14]. A control strategy to minimize EVs charging cost was studied. Their study is based on the pricing and the demand data of EVs energy. The results showed that the proposed method can be very effective in the regulation market [15]. Finally, a profitable business model for the EV fleet owners considering the change of electricity demand and their parking times by a heuristic algorithm was introduced [16].

The novelties of this paper include: the MG energy management considering uncertainty related to DG source and EVs, accurate charging and discharging scheduling of EVs considering relevant constraints and simultaneous reduction of operating emission and costs. For this purpose, the multi-objective particle swarm optimization (MOPSO) algorithm is used.

The rest of the paper is organized as follows: In Section 2, the problem is defined. The objective functions of cost, emission and constrains are introduced in this section. In Section 3, the modeling of uncertainties and scenario generations are discussed. In Section 4, the proposed MOPSO algorithm is introduced briefly. The description of the test MG is given in Section 5. The simulation approaches are presented in Section 6. Finally, Section 7 concludes this paper

2. Problem Formulations

Energy management of the MG means optimizing the use of sources with different approaches and constraints that can be defined as an optimization problem. One of the important issues in the management of resources in the MG is the reduction of costs and the environmental emissions [17]. The generation capacity of DGs should be determined to minimize energy costs and emissions considering operation limitations. Mathematical formulations for the DGs operation in a MG can be defined as follows:

2.1. Objective Functions

2.1.1. Operating Cost

One of the main goals of energy management in the MG and in the presence of EVs is the reduction of energy costs. The cost function is a combination of DG source cost and EVs cost of energy exchanged to the network. Therefore, the cost function is defined as follows [18]:

$$\begin{aligned}\mathrm{Min}\, f_1(X) &= \mathrm{Min}\sum_{\upsilon=1}^{N_S}\pi_\upsilon\sum_{t=1}^{T}\mathrm{cost}(t) = \mathrm{Min}\sum_{\upsilon=1}^{N_S}\pi_\upsilon\sum_{t=1}^{T}\Big(P_{Grid}(t)\times B_{Grid}(t)\\ &+\sum_{i=1}^{N_{DG}}(P_{DG}^{i}(t)\times B_{DG}^{i}+S_{DG}^{i}\,|U_{DG}^{i}(t)-U_{DG}^{i}(t-1)\,|)+\sum_{j=1}^{N_{EV}}P_{EV}^{j}(t)\times B_{EV}^{j}\Big),\end{aligned} \tag{1}$$

where, N_S is the number of random samples of operation conditions; π_υ is the probability of each sample; $P_{Grid}(t)$ and $B_{Grid}(t)$ are the power network and the price of electricity per hour during period t, respectively; N_{DG} is the number of DGs installed in the MG; $P_{DG}^{i}(t)$ and B_{EV}^{i} are power and electricity price of the ith DG during period t, respectively; S_{DG}^{i} is cost of the ith DG during period t; $U_{DG}^{i}(t)$ is a binary variable of shut down/startup of the ith DG during period t; N_{EV}

is the number of EVs; $P_{EV}^{j}(t)$ and $B_{EV}^{j}(t)$ are the power and the electricity price of charge and discharge of the *j*th EV in the network during period *t*, respectively, and T, is total number of hours (*t = 1, 2, . .,24).*

2.1.2. Emission

Another challenge of the management issue in the MG is the environmental emission. The most important emissions associated with DG source in MGs are Carbon dioxide (CO_2), Sulfur dioxide (SO_2) and Nitrogen oxides (NO_x). As a result, the emission function is defined as follows [19]:

$$\begin{aligned}\text{Min}\, f_2(X) &= \text{Min}\sum_{\upsilon=1}^{N_S}\pi_\upsilon \sum_{t=1}^{T} Emission(t)\\ &= \text{Min}\sum_{\upsilon=1}^{N_S}\pi_\upsilon \sum_{t=1}^{T}\left\{P_{Grid}(t)\times E_{Grid} + \sum_{i=1}^{N_{DG}} P_{DG}^{i}(t)\times E_{DG}^{i} + \sum_{j=1}^{N_{EV}} P_{EV}^{j}(t)\times E_{EV}^{j}\right\},\end{aligned} \tag{2}$$

where, E_{DG}^{i}, E_{EV}^{j} and E_{Grid} are represent the amount of pollutants emission in kg/MWh caused by the i*th* DG, the j*th* EV and the network, respectively. These emission variables are as follows:

$$E_{DG}^{i} = Co_{2_{DG}}^{\;i} + So_{2_{DG}}^{\;i} + No_{X_{DG}}^{\;i}, \tag{3}$$

where, $Co_{2_{DG}}^{\;i}$, $So_{2_{DG}}^{\;i}$ and $No_{X_{DG}}^{\;i}$ are the amounts of CO_2, SO_2 and NO_x from the i*th* DG sources, respectively. The same relations can be applied to EVs as follows:

$$E_{EV}^{j} = Co_{2_{EV}}^{\;j} + So_{2_{EV}}^{\;j} + No_{X_{EV}}^{\;j}, \tag{4}$$

where, $Co_{2_{EV}}^{\;j}$, $So_{2_{EV}}^{\;j}$ and $No_{X_{EV}}^{\;j}$ are the amounts of CO_2, SO_2 and NO_x from the j*th* EV, respectively.

$$E_{Grid} = Co_{2_{Grid}} + So_{2_{Grid}} + No_{X_{Grid}}, \tag{5}$$

where, $Co_{2_{Grid}}$, $So_{2_{Grid}}$ and $No_{X_{Grid}}$ are the amounts of CO_2, SO_2 and NO_x from the MG, respectively.

Reducing the cost of the energy production leads to an increase in environmental emission, and vice versa. This means that reduce cost and emission is impossible to simultaneously. As a result, the operation point must be chosen so that cost and emission are minimized to the lowest level.

2.2. Constrains

2.2.1. Power balance

The total power generated by DGs and EVs discharge and power purchased from the network should be equal to the sum of the load demands, the power used to charge EVs and the total power losses. The power balance is as equation (6):

$$P_{Grid}(t)+\sum_{i=1}^{N_{DG}}P_{DG}^{i}(t)+\sum_{j=1}^{N_{EV}}P_{EV\_Dch}^{j}(t)=D_t+\sum_{j=1}^{N_{EV}}P_{EV\_ch}^{j}(t)+Loss(t), \quad (6)$$

where, $P_{EV\_ch}^{j}(t)$ and $P_{EV\_Dch}^{j}(t)$ are the power charge and discharge of the *jth* EV, respectively; D_t is the load demand, and *Loss(t)* is the total power losses of power system during period *t*.

2.2.2 DGs Units Power Limitations

All the DGs have an upper and a lower limitation for their power generated as shown in equation (7):

$$P_{DG\_\min}^{i}\le P_{DG}^{i}(t)\le P_{DG\_\max}^{i}, \quad (7)$$

where, $P_{DG-\min}^{i}$ and $P_{DG-\max}^{i}$ are the minimum and maximum power limits of DG at time *t*.

2.2.3. Network Exchanged Power Limitation

The amount of electric power exchanged with the upstream power grid is limited as follows:

$$P_{Grid}(t)\le P_{Grid\_max}, \quad (8)$$

where, $P_{Grid}(t)$ is the amount of energy exchanged to the network, and P_{Grid_max} is the maximum power exchanged to the network.

2.2.4 EVs Constrains

In each programming period, the charge and discharge of EVs batteries cannot be done simultaneously as shown in equation (9).

$$A^{j}(t)+B^{j}(t)\le 1,\;\; A,B\in\{0,1\},\;\forall j\in\{1,\dots,N_{EV}\},\;\forall t\in\{1,\dots,T\} \quad (9)$$

where, $A^{j}(t)$ and $B^{j}(t)$ are the binary variables that show the charge and discharge mode of the j*th* EV in during period *t*. The charge and discharge rate of each EVs battery is limited as follows:

$$P_{EV\_ch}^{j}(t)\le P_{ch\_\max}^{j}\times A^{j}(t),\quad \forall j\in\{1,\dots,N_{EV}\},\;\forall t\in\{1,\dots,T\} \quad (10)$$

$$P_{EV\_Dch}^{j}(t)\le P_{Dch\_\max}^{j}\times B^{j}(t),\;\forall j\in\{1,\dots,N_{EV}\},\;\forall t\in\{1,\dots,T\} \quad (11)$$

where $P_{ch\_\max}^{j}$ and $P_{Dch\_\max}^{j}$ are the maximum charge and discharge rate of the *j*th EV. Further, the amount of energy stored in the EV batteries shall not be less than or greater than specified amounts as expressed in (12) and (13).

$$E_S^{j}(t)\le\psi_{max}^{j},\quad \forall j\in\{1,\dots,N_{EV}\},\;\forall t\in\{1,\dots,T\} \quad (12)$$

$$E_S^j(t) \geq \psi_{\min}^j, \quad \forall j \in \{1,...,N_{EV}\}, \forall t \in \{1,...,T\} \tag{13}$$

where, $E_S^j(t)$ is the charge state of the j*th* EV at *t* period (kWh), and ψ_{min}^j and ψ_{max}^j are the minimum and maximum battery charge level (kWh), respectively. These limitations are considered to prevent shortening battery life. The $E_S^j(t)$ is calculated as equation (14).

$$E_S^j(t) = E_S^j(t-1) + \eta_{ch}^j \times P_{EV\_ch}^j(t) - E_{trip}^j(t) - \frac{1}{\eta_{Dch}^j} \times P_{EV\_Dch}^j(t), \tag{14}$$

$$\forall j \in \{1,...,N_{EV}\}, \forall t \in \{1,...,T\}$$

where, $E_S^j(t-1)$ is the remaining energy from previous period; $E_{trip}^j(t)$ is the power consumption for one-hour trip to constant speed, and η_{ch}^j and η_{Dch}^j are EVs charge and discharge efficiency.

3. Scenario Based Stochastic Model of system

Basically, the variables in a MG have uncertainties and they must be considered in a model to confirm the results obtained from studies. The reasons for uncertainty can be due to random nature variables or inaccuracy in measuring. Therefore, the proper Probability Density Function (PDF) should be chosen for each variable to create different scenarios. Obviously, load, as the most probable variable of uncertainty, plays a very important role in the performance of problems associated with load change. For this reason, a normal PDF is widely used for load change [20]. The PDF for load changes is expressed as equation (15).

$$f(\mathrm{P}_L) = \frac{1}{\sqrt{2\pi \times \sigma_{PL}}} \exp(-\frac{(P_L - \mu_{PL})^2}{2 \times \sigma_{PL}^2} \tag{15}$$

where, P_L is the load power; μ_{PL} and σ_{PL} are the mean and the variance of load power, respectively.

The power of a photovoltaic array depends on the intensity of solar radiation at the installed location [21]. For this reason, a Beta PDF is used to the power production of a PV array. So, the PV power output is expressed as a function of radiation to respect to the power curve of sun radiation as equation (16).

$$f_B(\mathrm{P}_{PV}) = \begin{cases} \frac{\Gamma(\alpha+\beta)}{\Gamma(\alpha).\Gamma(\beta)} (A_c \times \gamma \times \xi)^{\alpha-1} (1-(A_c \times \gamma \times \xi))^{\beta-1} & if \quad P_{PV} \in [0, P_{PV}(\xi)], \\ 0 & otherwise \end{cases} \tag{16}$$

where, ξ represents the amount of solar radiation in kW/m^2; α and β are the parameters of cumulative PDF; $P_{PV}(\xi)$ represents the power output of PV in kW; γ is the PV efficiency, and A_c is the area of arrays in m^2.

The wind speed is described as a Weibull distribute function to determine the power of a WT as equation (17) [22].

$$f_w(v) = \begin{cases} \frac{k}{c} \times (\frac{v}{c})^{k-1} \exp(-(\frac{v}{c})^k), & v \geq 0 \\ 0 & otherwise \end{cases}, \tag{17}$$

where, v is the wind speed in m/s, and k and c are the shape factor and the scale parameter, respectively. The distributions take different shapes with different values of k and c.

The connection of EVs to the MG, creates a load type with a new definition. Thus, EVs can be used as the energy consumers during charging and electric power generators during discharging. Assuming the presence of EVs is random and there are no available data for their behavior. The uncertainty associated with the power produced and consumed by vehicles in charging stations is modeled using fuzzy logic with triangular membership functions that is described as equation (18) and (19).

$$\mu_{char}(P_{EV}) = ([1 - \lambda] \times P_{EV}^r, P_{EV}^r, [1 + \lambda] \times P_{EV}^r); \tag{18}$$

$$\mu_{dchar}(P_{EV}) = -([1 - \lambda] \times P_{EV}^r, P_{EV}^r, [1 + \lambda] \times P_{EV}^r). \tag{19}$$

where, P_{EV}^r and λ are the power rated and the uncertainty coefficient of EV in charging stations, respectively [23].

In this paper, the Roulette Wheel method is used to generate scenarios for the energy management of the MG source. Hence, the PDFs is categorized into seven levels, according to the degree of accuracy considered for the solutions. Then a random number with normal distribution is created within interval [0 1], and according to the obtained value, one part of the Roulette Wheel is selected for indicating the amount of variability. For example, as shown in Fig. 1a, a normal PDF for load values has been selected, which can be divided to seven levels. π_1 to π_7 are the probability of each level as depicted in Fig. 1b, by the random selection of a number in the range 0 to 1, one of the levels from π_1 to π_7 is selected [24].

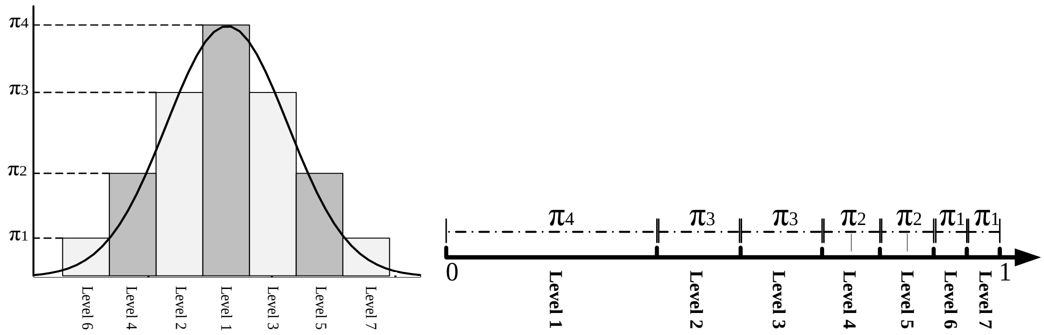

(a) (b)

Fig. 1. (a.) PDF for load changes and (b.) Roulette wheel mechanism

4. Multi-objective Particle Swarm Optimization Algorithm (MOPSO)

The MOPSO algorithm is a developed version of the Particle Swarm Optimization (PSO) algorithm, which presented by CoelloCoello in 2004. In this algorithm, the particles are randomly dispersed in search area and objective functions are calculated for each particle. After that, the particles are evaluated according to the objective function's values, and the non-dominated solutions are stored in the repository [25]. In the MOPSO, particles are updated as equations (20) and (21):

$$V_k(t+1) = D_d \times w \times v_k(t) + c_1 \times r_1 \times (x_k^{Pbest}(t) - x_k(t)) + c_2 \times r_2 \times (Rep_k(t) - x_k(t)); \tag{20}$$

$$x_k(t+1) = x_k(t) + v_k(t+1). \tag{21}$$

where, v_k is the velocity of particle *k*; D_d is damping coefficient; *w* is weighting factor, r_1 and r_2 are random numbers between 0 and 1. c_1 and c_2 are impression coefficients, and $Rep_k(t)$ is a solution selected from the repository in each iteration. For the subsequent iterations the $x_k^{Pbest}(t)$ is updated as follows:

(1) If dominates $x_k^{Pbest}(t)$ then $x_k^{Pbest}(t+1) = x_k(t+1)$.

(2) If the current dominates $x_k(t+1)$ then $x_k^{Pbest}(t+1) = x_k^{Pbest}(t)$.

(3) If no one dominates the other, then one of them is randomly selected to be the $x_k^{Pbest}(t+1)$.

This step is repeated until the best answer is obtained. The flowchart of the MOPSO algorithm is shown in Fig. 2. Here, the MOPSO algorithm is used to minimize the operation cost and the emissions.

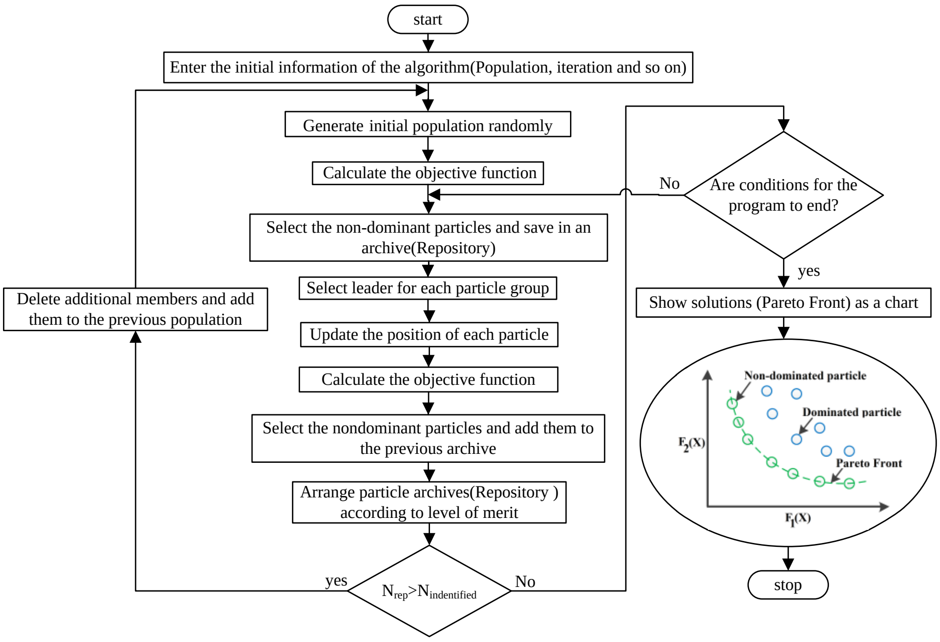

Fig. 2. MOPSO algorithm flow chart

5. Simulation Results

In the previous sections, the energy management of DGs and EVs with the aim of reducing energy costs and environmental pollution is formulated. In this section, a case study of a typical low-voltage network-connected MG is presented in which the proposed energy management scheme is implemented. The low-voltage grid-connected MG consists of different types of power sources includes: photovoltaic array (PV), wind turbine (WT), micro turbine (MT), fuel cell (FC) and electrical vehicles (EVs). The single diagram of the MG is shown in Fig..3.

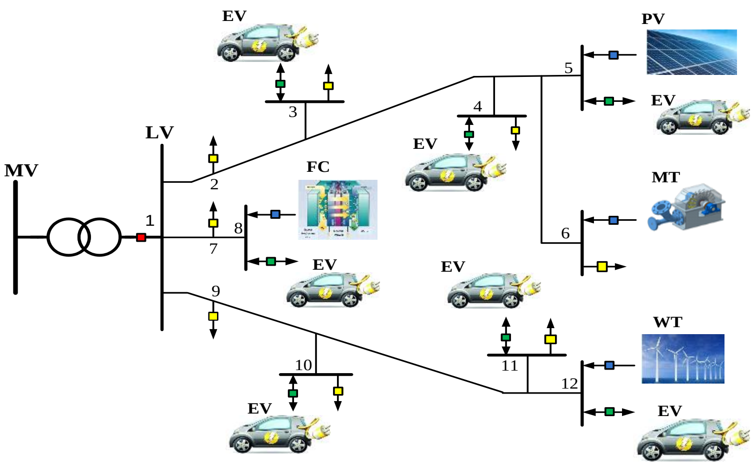

Fig. 3. The MG under study with electrical vehicle parking lots

It is assumed that all DG units are working at unit power factor, so that no reactive power trading exists. Moreover, according to the decisions taken in the microgrid central controller (MGCC), proper power trading between the MG and the market (utility) can be established at each hour of the day. In Fig. 4, the load curve is shown in the studies of daily period. Total energy consumption for load in the MG for 24 hours is about 94803 kWh and the peak load is 5072 kW. Also, the output curves of power, PV and WT are shown in Fig. 5.

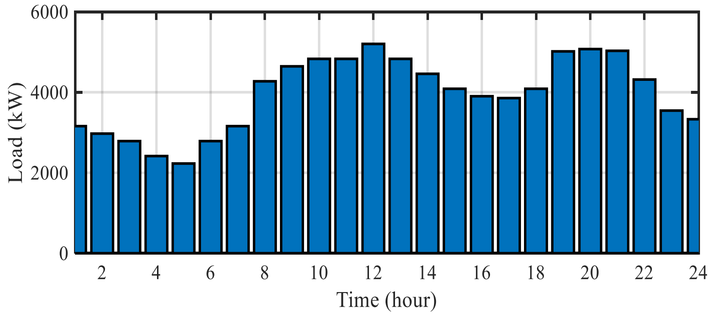

Fig. 4. Load curve for 24 hours in MG

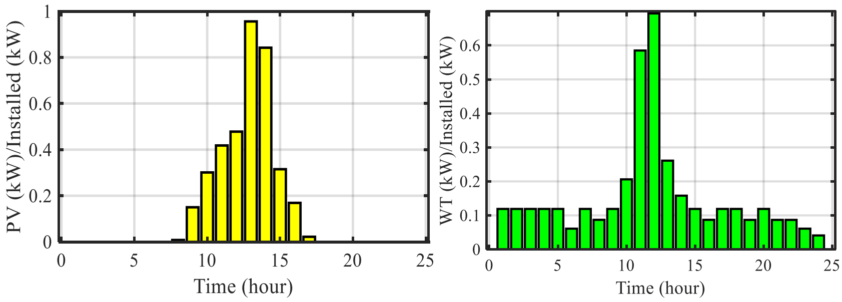

Fig. 5. PV and WT power curves

The considered MG incorporates 1000 EVs into seven parking lots whose driving patterns are chosen by statistical data as used in [26]. The information includes: the travel time of each EV, the start time, the end time of the trip and the average distance travelled. Thus, the EVs are divided into seven groups, namely, EI, EI2, EO, EO2, SP, OU and TR, as shown in Table 1.

Table 1

The EVs driving pattern for seven EV groups for 24 hours

Group name	Number of EVs in group	Possible times of connecting to the network
EI1	200	01:00-06:00,08:00-15:00,17:00-24:00
EI2	200	01:00-06:00,08:00-15:00,17:00-19:00
EO1	100	01:00-05:00,11:00-14:00,17:00-24:00
EO2	200	01:00-05:00,11:00-15:00,17:00-19:00,22:00-24:00
SP	150	01:00-09:00,13:00-18:00,22:00-24:00
OU	100	01:00-06:00,08:00-15:00,20:00-24:00
TR	50	01:00-06:00,12:00-15:00,20:00-22:00

It is assumed that the EV owners drive at a constant speed and the energy consumption of each EV is 3 kWh per hour. In simulation part, EVs of Nissan Leaf type with a 24-kWh battery capacity is used. The maximum charge and discharge rate for each EV is 4 kWh and also depth of discharge (DOD) is considered 25% and the maximum state of charge (SOC) is 85%. Battery capacity. Also, each EV can be energy exchange a maximum of 4 kWh with the upstream network. The energy stored in the batteries should be sufficient to cover the travel distance. The cost of energy produced and emission of each DG and EVs in the MG with their technical limitations are presented in Table 2 [27].

Table 2

Cost and emission of DGs and electrical vehicles

Unit	Cost		Emission		
	S ($/MWh)	Bid ($/MWh)	NO_X (kg/MWh)	SO_2 (kg/MWh)	CO_2 (Kg/MWh)
PV	0	2.584	0	0	0
WT	0	1.073	0	0	0
FC	1.65	0.294	0.0075	0.003	460
MT	0.96	0.457	0.1	0.0036	720
EV	0	0.24	0.014	0.001	41.9

According to Table 2, PV and WT energy characteristics can be distinguished by their lack of emission, while MT and FC sources have relatively high emissions. The total cost includes: the sum of initial maintenance, the DGs fuel and the EVs parking cost. The cost of energy exchanged with the network in 24 hours is given in Table 3. According to this table, the price of electricity at low consumption hours is cheaper than at the peak times. Therefore, the energy producers of DGs and EVs reduce energy production at low consumption hours and increase production at peak times. The total cost of the network in the absence of DGs and EVs is about 20454$.

Table 3

The price of electricity per hour [28]

Time(h)	**1**	**2**	**3**	**4**	**5**	**6**	**7**	**8**
Price ($/kWh)	0.033	0.027	0.02	0.017	0.017	0.029	0.033	0.054
Time(h)	9	10	11	12	13	14	15	16
Price ($/kWh)	0.215	0.572	0.572	0.572	0.572	0.572	0.286	0.279
Time(h)	17	18	19	20	21	22	23	24
Price ($/kWh)	0.086	0.059	0.05	0.061	0.181	0.077	0.043	0.037

In this paper, time of use (TOU) pricing method is used for electric power exchanged by upstream network. Simulations are done in three cases. In the first case, the optimal management of MG with the aim of reducing costs is considered. In the second case, the optimization is done with the goal of reducing emissions, and finally, in the third one, simultaneous reduction of cost and emissions is studied. To achieve the optimal energy management of MG in the first and the second cases, particle swarm optimization (PSO) and genetic algorithm (GA) are used [29, 30]. In the third case, the MOPSO and multi-objective genetic algorithm (NSGAII) are used to reduce cost and emission simultaneously [31, 32]. For each case, 10 different scenarios are defined and optimizations are done for all scenarios. The scenarios are generated by the roulette wheel mechanism and using PDFs defined for each resource, loads and vehicles. The algorithms are performed 20 times for each scenario. To perform the optimization, 1000 scenarios were generated by the roulette wheel method, but the results of 10 random scenarios are chosen and explained in comparison.

5.1. First Case (Minimizing the Cost of Operation)

In the first part of the simulation, the energy management of DG sources and EVs in the MG under study is performed with the aim of reducing the operating cost by using PSO and GA algorithms. The amount of energy generated by DGs and energy produced of EVs charge and discharge is determined by the algorithms in such a way to minimize the cost of the operation. The best, worst, average and standard deviations of solutions are calculated for each scenario. The results are given in Table 4.

Table 4

Simulation results in the first case using PSO and GA algorithms in 10 scenarios

Scenario	Best ($)		Worst ($)		Average ($)		Standard deviation ($)		Simulation time (s)	
Algorithm	GA	PSO	GA	PSO	GA	PSO	GA	PSO	GA	PSO
S1	9812	9764	9856	9784	9841	9773	22.36	7.42	451	374
S2	10186	10123	10248	10141	10205	10137	29.17	7.76	445	381
S3	8833	8793	8825	8805	8796	8800	24.36	6.32	446	376
S4	9875	9806	9913	9818	9891	9810	26.51	6.38	450	382
S5	9759	9719	9810	9731	9789	9726	23.72	6.84	453	377
S6	10061	9923	9948	9948	10029	9929	25.86	7.83	451	378
S7	8904	8839	8949	8851	8932	8844	30.11	6.29	448	376
S8	8984	8901	9136	8926	9118	8909	27.21	7.51	450	381
S9	9621	9568	9677	9578	9646	9572	26.90	6.81	449	380
S10	9713	9647	9762	9662	9738	9653	28.13	7.57	452	375

The numerical results reveal that the PSO algorithm has a lower cost and profitability than the GA algorithm. For example, the lowest cost is 8793$ and 8833$ for PSO and GA algorithms, respectively, is obtained in the 3*th* scenario. In this scenario, the average cost is 9515$ and 9599$ for PSO and GA algorithms, respectively. The differences between the best and the worst solutions are low for the PSO algorithm in the *10th* scenarios. For this reason, the standard deviation is small. The small amount of standard deviation for the PSO algorithm indicates the high accuracy of this algorithm. As a result, the PSO algorithm is better than the

GA algorithm due to more efficient arrangement and scheduling of vehicles at the charging station. Also, the convergence time in the GA algorithm is high. But the PSO algorithm has a good convergence time, lower cost and greater profitability. The percentage of the profitability for 7 groups of EVs is presented in Fig. 6.

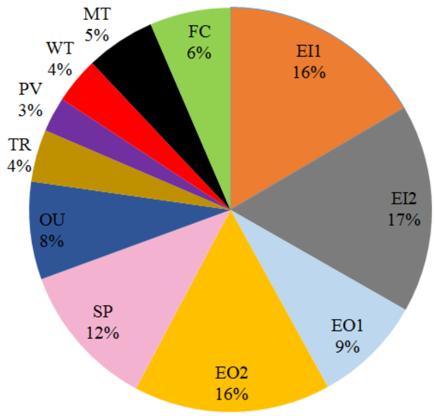

Fig. 6. The percentage of the profitability for EV groups and DGs

Based on the obtained results, in the first case, the total profitability of the network in the presence of DG sources and EVs is about 95083$, of which 77421$ (81.4%) is due to the existence of EVs and 17662$ (about 18%) is attributed to DGs.

5.2. Second Case (Minimizing the Emission)

In the second case, the energy management of DGs and EVs in the MG is carried out by PSO and GA algorithms aiming to reduce emission. In this part of the optimization, the algorithms should provide a schedule for utilizing DGs and EVs so that the emissions are minimized. The results of the 10 scenarios are shown in Fig. 7.

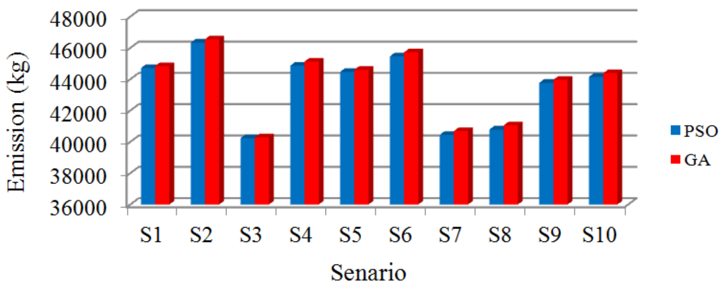

Fig. 7. Emission values for 10 scenarios in second case

As shown in Fig. 7, the amount of emission obtained by the PSO algorithm in all scenarios is less than that of GA algorithm. The lowest emission for PSO and GA is in the *3th* scenario and the maximum amount is witnessed in the *2th* scenario. Therefore, it can be concluded that by increasing the load, the emissions increase. According to the results, PV and WT resources produce their maximum power output in order to minimize the emissions. On the other hand, MT and FC have the lowest share in the power generation. Due to lower emissions of EVs than MT and FC, the EVs have a larger share of energy exchange. The operating schedule moves toward supplying the demand by more charging and discharging of EVs in order to reduce emissions. Because the cost is not considered in the objective function for the second case of the simulation, EVs have contributed more in supplying the demand.

5.2.3. Third Case (Minimizing the Cost and Emission Simultaneously)

In the third case of simulations, the energy management of DG resources and EVs in the MG studies with the aim of reducing the cost and the emission simultaneously. For this purpose, two multi-objective algorithms, including the MOPSO and NSGAII are applied to find the optimal operating point of resources and EVs at each hour. The results are provided in Tables 5.

Table 5

Simulation results in the third case using a MOPSP algorithm in 10 scenarios

Scenario	algorithm	Simulation Time (S)	Best ($)		Worst ($)		Average ($)	
			Cost ($)	Emission (kg)	Cost ($)	Emission (kg)	Cost ($)	Emission (kg)
S1	MOPSO	616	12693	56786	12915	57270	12705	56802
	NSGAII	714	12756	57396	13108	58104	12892	57565
S2	MOPSO	639	13160	58857	13386	59355	13178	58872
	NSGAII	720	13242	59584	13630	60415	13369	59695
S3	MOPSO	621	11431	51104	11623	51538	11440	51119
	NSGAII	724	11406	51580	11737	52413	11523	51727
S4	MOPSO	625	12748	56982	12960	57463	12753	56996
	NSGAII	730	12838	57765	13184	58491	12957	57859
S5	MOPSO	628	12635	56478	12845	56963	12644	56495
	NSGAII	728	12687	57087	13047	57833	12824	57262
S6	MOPSO	625	12900	57737	13131	58220	12908	57751
	NSGAII	713	13007	58525	13381	59313	13138	58666
S7	MOPSO	626	11491	51370	11683	51799	11497	51379
	NSGAII	720	11575	52084	11902	52757	11701	52248
S8	MOPSO	616	11571	51806	11782	52246	11582	51826
	NSGAII	730	11679	52553	12151	53344	11945	52696
S9	MOPSO	632	12438	55589	12643	56068	12444	55606
	NSGAII	732	12507	56279	12870	57049	12636	56425
S10	MOPSO	635	12541	56077	12754	56549	12549	56092
	NSGAII	724	12627	56817	12983	57549	12757	56964

The responses in ideal Pareto front should be distributed equally. If the dominant particles are distributed uniformly, then the algorithm is more accurate in choosing the optimal response. As an example, the Pareto fronts in the *1th* scenario for the two algorithms are shown in Fig. 8.

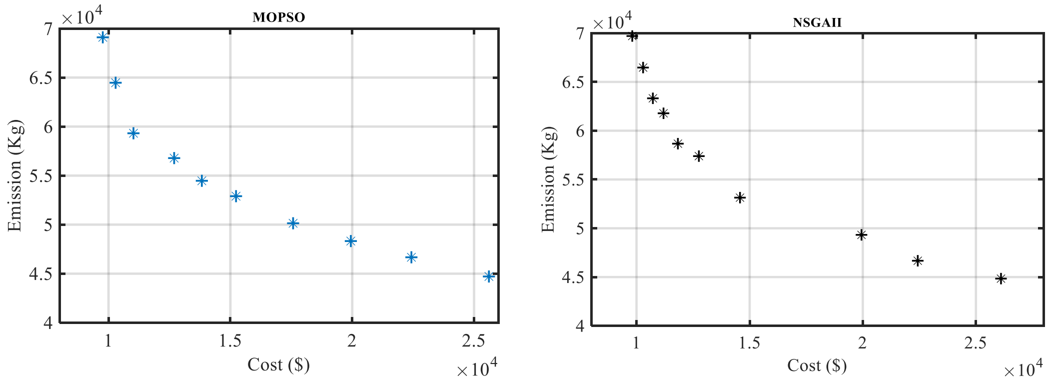

(a.) (b.)

Fig. 8. Pareto fronts of (a.) MOPSO, (b.) NSGAII algorithms

In Fig. 8, the Pareto front is drawn for the 10 dominant particles of MOPSO and NSGAII algorithms. If the dominant particles are uniformly distributed, choosing the best response from the Pareto front is possible. In order to evaluate the results of simulations in the third case more accurately, the metric distance criteria are calculated for the algorithms, which is expressed as follows:

$$s=\sqrt{\frac{1}{N_k-1}\sum_{i=1}^{N_k}(\bar{d}-d_i)^2}, \tag{22}$$

In equation (22), N_k is the number of particles, d_i is the distance between the k*th* particle and the nearest neighbor and d is the average distances, which are calculated as follows:

$$d_i=\min\left\{\sum_{m=1}^{N_{obj}}\frac{\left|f_m(x_i)-f_m(x_j)\right|}{f_{m.\max}-f_{m.\min}}\right\}; \tag{23}$$

$$\bar{d}=(\sum_{i-1}^{N_k}d_i)/N_k. \tag{24}$$

where, $f_{m.\min}$ and $f_{m.\max}$ are minimum and maximum solutions, respectively. The lower value of metric distance means that the solutions in the Pareto solution are more distributed, and the zero value for the metric distance means that all solutions in the Pareto solution set are equally spaced.

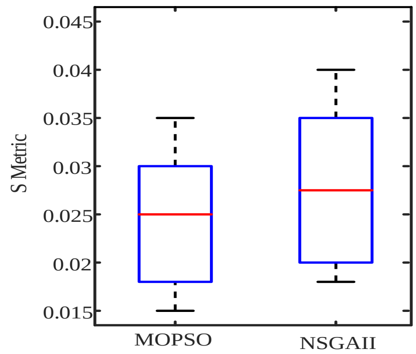

Fig. 9. Metric distance for multi objective algorithms

In Fig. 9, the upper and lower horizontal lines represent the boundary values. The square box contains half the metric distance and the red line in the square box represents the average values of the metric distance. By comparing the algorithms, the proposed method of the MOPSO algorithm has the minimum average value and the minimum metric distance. The lower horizontal line of the MOPSO algorithm is lower than that of the NSGAII algorithm. As a result, compared to the other algorithms, this algorithm has a better performance in finding uniform distribution solutions and Pareto front.

6. Conclusion

This paper focuses on the energy management of DG sources and EVs in the grid-connected MG to reduce the operating cost and emissions in the presence of uncertainties. In this study, the uncertainties of power generation of DGs, EVs and network load are considered. Thus, new scenario-based objective functions are introduced which have been formulated in such a way to encompass all the uncertainties weighted according to their probability of occurrence. In order to achieve the most accurate results, the simulations are done in three cases with 10 scenarios generated by the roulette wheel mechanism. The modified version of the single-objective function GA and PSO algorithm as multi-objective function NSGAII and MOPSO are used to solve the optimization problem. Performing 20 times of algorithm run for each scenario, the lowest value of the objective function and the standard deviation is obtained for the PSO algorithm. In the third case, the cost and emission reductions are achieved simultaneously by using MOPSO and NSGAII algorithms. The simulation results indicate the good performance of the proposed PSO and the MOPSO algorithms in each scenario. The minimum amount of the objective functions in the third case is obtained for the MOPSO algorithm.

R E F E R E N C E S

[1]. *A. Horhoianu, and M. Eremia*, "Smart grid energy management systems: Control mechanisms for electricity demand", UPB Scientific Bulletin, Series C: Electrical Engineering and Computer Science., **vol. 78**, 2016, pp. 293_307.

[2]. *S. Gheorghe, N.Golovanov, G.C.Lazaroiu and R.Porumb*, "integration of renewable sources and improvement of power quality", International Conference on Control Systems and Computer Science (CSCS), **vol. 79**, Iss. 1, May. 2017, pp. 29_31.

[3]. *K. Seddig, P. Jochem, and W. Fichtner*, "Integrating renewable energy sources by electric vehicle fleets under uncertainty", Energy., **vol. 141**, no. 1, Dec. 2017, pp. 2145_53

[4]. *S. Khan, K. Mehmood, Z. Haider, S. Bukhari, SJ. Lee, M. Rafique, and CH. Kim*, "Energy management scheme for an ev smart charger V2G/G2V application with an EV power allocation technique and voltage regulation, "Applied Sciences., **vol. 8**, no. 4, Jun. 2018, p. 648.

[5]. *Ş. Andreea, and E. Mircea*, "Trends on integrating the electric vehicles in distribution networks", U.P.B. Sci. Bull., Series C, **vol. 77**, Iss. 1, Jan. 2015, pp. 197_204.

[6]. *E. Mirmoradi, and H. Ghasemi*, "Market clearing with probabilistic spinning reserve considering wind uncertainty and electric vehicles", International Transactions on Electrical Energy Systems., **vol. 26**, no. 3, Mar. 2016pp. 525_38.

[7]. *S. Falahati, SA. Taher, and M. Shahidehpour*, "A new smart charging method for EVs for frequency control of smart grid", International Journal of Electrical Power & Energy Systems., **vol. 83**, no. 1, Dec. 2016, pp. 458_69.

[8]. *Z. Wang, Q. Zhu, M. Huang, and B. Yang*, "Optimization of economic/environmental operation management for microgrids by using hybrid fireworks algorithm", International Transactions on Electrical Energy Systems., **vol. 27**, no. 12, Dec. 2017 p. e2429.

[9]. *S. Shojaabadi, S. Abapour, M. Abapour, and A. Nahavandi*, "Simultaneous planning of plug-in hybrid electric vehicle charging stations and wind power generation in distribution networks considering uncertainties", Renewable energy., **vol. 99**, no. 1, Dec. 2016, pp. 237_52.

[10]. *T. Praveen Kumar, N. Subrahmanyam, and M. Sydulu*, "Power Flow Management of the Grid-Connected Hybrid Renewable Energy System: A PLSANN Control Approach", IETE Journal of Research., **vol. 26**, no. 1, Jan. 2019, pp. 1_6.

[11]. *MF. Zia, E. Elbouchikhi, and M. Benbouzid*, "Microgrids energy management systems: A critical review on methods, solutions, and prospects", Applied energy., **vol. 222**, no. 15, Jul. 2015, pp.1033_1055.

[12]. *N. Erdogan, F. Erden, and M. Kisacikoglu*, "A fast and efficient coordinated vehicle-to-grid discharging control scheme for peak shaving in power distribution system", Journal of Modern Power Systems and Clean Energy., **vol. 6**, no. 3, May. 2018, pp. 555-66.

[13]. *J. Kaur, YR. Sood, and R. Shrivastava*, "Optimal Resource Utilization in a Multi-Microgrid Network for Tamil Nadu State in India", IETE Journal of Research., **vol. 5**, no. 1, Apr. 2019, pp. 221_31.

[14]. *J. Wu, Z. Wu, F. Wu, and X. Mao*, "A power balancing method of distributed generation and electric vehicle charging for minimizing operation cost of distribution systems with uncertainties", Energy Science & Engineering., **vol. 5**, no. 3, Jun. 2017, pp. 167_79.

[15]. *E. Mengelkamp, J. Gärttner, K. Rock, S. Kessler, L. Orsini, and C. Weinhardt*, "Designing microgrid energy markets: A case study: The Brooklyn Microgrid", Applied Energy., **vol. 210**, no. 1, Jan. 2018, pp. 870_80.

[16]. *M. Kahlen, K. Valogianni, W. Ketter, and J. Van Dalen*, "A profitable business model for electric vehicle fleet owners", International Conference on Smart Grid Technology, Economics and Policies (SG-TEP) IEEE., **vol. 3**, no. 1, Dec. 2012, pp. 1_5.

[17]. *A. Horhoianu, and M. Eremia*, "Evaluation of an industrial microgrid using homer software", UPB Scientific Bulletin, Series C: Electrical Engineering and Computer Science., **vol. 79**, no. 4, 2017, pp. 193_210.

[18]. *M. Ghahramani, M. Nazari-Heris, K. Zare, and B. Mohammadi-Ivatloo*, "Energy Management of Electric Vehicles Parking in a Power Distribution Network Using Robust Optimization Method" Journal of Energy Management and Technology., **vol. 2**, no. 3, Sep. 2018, pp. 22_30.

[19]. *A. Rabiee, M. Sadeghi, and J. Aghaei*, "Modified imperialist competitive algorithm for environmental constrained energy management of microgrids," Journal of cleaner production., **vol. 202**, 2018, pp. 273_292.

[20]. *H. Shokouhandeh*, and *M. Jazaeri*, "An enhanced and auto-tuned power system stabilizer based on optimized interval type-2 fuzzy PID scheme," International Transactions on Electrical Energy Systems., **vol. 28**, no. 1, p. e2469.

[21]. *V. Dumbrava, G.C. Lazaroiu, S. Leva, G. Balaban, M. Teliceanu, and M. Tirsu*, "Photovoltaic production management in stochastic optimized microgrids", UPB Scientific Bulletin, Series C: Electrical Engineering and Computer Science., **vol. 79**, no. 1, 2017, pp. 225_244.

[22]. *P. Wais*, "Two and three-parameter Weibull distribution in available wind power analysis," Renewable energy., **vol. 103**, no. 1, Apr. 2017, pp. 15_29.

[23]. *S. Faddel, AT. Al-Awami, and MA. Abido*, "Fuzzy optimization for the operation of electric vehicle parking lots, "Electric Power Systems Research., **vol. 145**, no. 1, Apr. 2017, pp. 166_74

[24]. *A. Lipowski, and D. Lipowska*, "Roulette-wheel selection via stochastic acceptance", Physica A: Statistical Mechanics and its Applications., **vol. 391**, no. 6, Mar. 2012, pp. 2193_6.

[25]. *N. Borges, J. Soares, and Z. Vale*, "Multi-objective Particle Swarm Optimization to Solve Energy Scheduling with Vehicle-to-Grid in Office Buildings Considering Uncertainties," IFAC-Papers on Line., **vol. 50**, no. 1, Jul. 2017, pp. 3356_61.

[26]. *F. Najibi, and T. Niknam*, "Stochastic scheduling of renewable micro-grids considering photovoltaic source uncertainties. Energy conversion and management", Energy conversion and management., **vol. 98**, 2015, pp. 484_499.

[27]. *M. Heidari, T. Niknam, M. Zare, and S. Niknam*, "Integrated battery model in cost-effective operation and load management of grid-connected smart nano-grid", IET Renewable Power Generation., **vol. 13**, no. 7, 2019, pp. 1123_1131.

[28]. *A. Moghaddam, A. Seifi, T. Niknam, and M Pahlavani*, "Multi-objective operation management of a renewable MG (micro-grid) with back-up micro-turbine/fuel cell/battery hybrid power source," Energy., **vol. 36**, no. 11, 2011, pp. 6490_6507.

[29]. *D. Laurentiu, and P. Cornel*, "Improving PSO based algorithms with the domain-shrinking technique for electromagnetic devices optimization", U.P.B. Sci. Bull., Series C, **vol. 80**, Iss. 1, Jan. 2018, pp. 179_90.

[30]. *CH. Dharmakeerthi, N. Mithulananthan, and TK. Saha*, "A comprehensive planning framework for electric vehicle charging infrastructure deployment in the power grid with enhanced voltage stability," International Transactions on Electrical Energy Systems., **vol. 25**, no. 6, Jun. 2015, pp. 1022_40.

[31]. *LI. Peng, and YU. Jilai*, "Identification of charging behavior characteristic for large-scale heterogeneous electric vehicle fleet," Journal of Modern Power Systems and Clean Energy., **vol. 6**, no. 3, May. 2018, pp. 567_81

[32]. *G. Kyriakarakos, AI. Dounis, KG. Arvanitis, and G. Papadakis*, "A fuzzy cognitive maps–petri nets energy management system for autonomous polygeneration microgrids", Applied Soft Computing, **vol. 12**, no. 12, Dec. 2012, pp. 3785_97.